INTERNATIONAL JOURNAL OF ADVANCED RESEARCH
International Peer-Reviewed Research Journal
ISSN (Online): 3106-7980 | ISSN (Print): 3106-7972
Volume 3 • Issue 2 • April 2026

DIFFRACTION BY PERFECTLY ELECTRIC CONDUCTING (PEC) SLOT EMBEDDED NEAR ZERO INDEX (NZI) MATERIALS

M. Imran Shahzad[*1], Sania Shaheen[2], M. Saddique[3], Mudassar Hussain[4], Saeed Ahmed[5]

[*1,2,3]*Department of Physics, Federal Urdu University of Arts, Sciences and Technology, Islamabad, Pakistan,*
[4]*Department of Physics, NFC Institute of Engineering and Technology, Multan,Pakistan,*
[5]*Department of Electronics, Quaid-i-Azam University, Islamabad, Pakistan,*

[*1]ishahzad@fuuast.edu.pk, [2]sania.shaheen@fuuast.edu.pk, [3]msaddique@fuuast.edu.pk
[4]mudassar.hussain@nfciet.edu.pk, [5]saeedqau@gmail.com

DOI: https://doi.org/10.5281/zenodo.2368450

Keywords
Electromagnetic diffraction, Perfectly electric conducting, Near zero index materials

Article History
Received: *01 March 2026*
Accepted: *15 April 2026*
Published: *30 April 2026*

Copyright @Author
Corresponding Author: *
M. Imran Shahzad

Abstract
We present here an analytic theory which is developed for the electromagnetic diffraction from a perfect electic conductor (PEC) Slot embedded in near zero Material as host media. The diffracted field of a plane wave from a PEC slot placed in mu-near-zero (MNZ), epsilon-near-zero (ENZ) and mu and epsilon double-near-zero (DNZ). The problem was solved by using the Sommerfeld Green's function and Fresnel Integral. . The scattering width is evaluated as a function of observation angle for various combinations of relative permittivity and permeability approaching zero, with incidence angles of 30°, 60°, and 90°. The physical mechanisms responsible for this enhancement are attributed to the increased phase velocity, reduced spatial phase variation, and energy funnelling effects in near-zero index media. The angular width of the diffraction peak narrows as the slot width increases, providing a tunable parameter for beam shaping. The numerical results have been compared with available literature and are found in good agreement.

INTRODUCTION

We have exteded a known problem [1] which is considered, wherein an E-polarized far zone field diffracted by a slot that is perfectly conducting has been examined. In order to investigate EMR or EMP interconnected with devices and subsystems, it is necessary to understand the fundamental mechanism of the problem by which an electromagnetic plane wave enters an opening in a shielded enclosure. However, for aperture widths as small as one or two wavelengths, the formulas for distant zone fields might be found by using asymptotic approaches [2, 3]. Both the boundary conditions in the slot plane and the reciprocity principle are satisfied by these statements. The problem's direction was consistent with both the experimental and analytical findings. The edge approach provided a solution to the issue. The method employed by Schwarzschild [4], who initially thought of a slot as essentially consisting of two difiracting half-planes, is roughly comparable to this one. The Sommerfeld Green's function can be used to determine how each half plane will react to various excitations. It is possible to compute the fields diffracted by apertures of different forms by utilizing more than two half-planes and applying Babinet's duality principle. But the conversation here is limited to that time window. because Fresnel integrals and basic exponential functions can be used to

approximate the functions related to the edge technique. There are several uses for slots in communication systems, particularly in antennas. Slot antennas are widely utilized in a variety of real-world applications, including radar and satellite communications, spacecraft, aircraft, missiles, and typical desktop microwave sources for research. The primary benefits of slot antennas are their versatility, light weight, simplicity of design, ease of manufacture, high power capability, more control over the radiation pattern than line antennas, and broader bandwidth than microstrip patch antennas.

There have been viable research efforts in the field of meta-materials [1]-[5]. They are the artificial structures that exhibit unusual properties but not readily exist in nature. On the basis of real part of the values of refractive index, the optical meta-materials may be divided into two categories. The first one is negative refractive index while the other is near-zero index materials. The negative refractive index metamaterials are also known as â€˜left-handedâ€™ materials. They are artificial composites with negative effective value of refractive index and have sub-wavelength features [6]-[7]. The basic characteristics of the first type of metamaterials is the negative phase velocity of the plane waves, propagating in the negative index mediums [8]. They have many applications in the field of science such as super lens, the reversal of Snellâ€™s law, reduction of the size of patch antennas, invisible cloaking, perfect absorber and the photonic band gaps with averaged zero refractive index [9]-[14]. The second type of metamaterials having a near-zero refractive index have been thoroughly discussed in [15]. The electromagnetic ï¬•elds in this type of medias are dynamic in time but remain static in space. A remarkable work has been done for metamaterials with a near-zero refractive index (NZI) for visible and infrared wavelengths. Electromagnetic waves (EM) inside such materials have large phase velocity and experience no spatial phase change [15]-[17]. These type of materials have several applications such as super reflection [18], cloaking [18]-[20], funnelling [21] and tunnelling [22]-[24]. In scattered fields the use of near-zero index materials may give phase distribution from various geometries such as cylindrical shells, planar slabs and lenses with various exit faces.

Among the metamaterials, the near-zero constitutive parameters are of great interest [25]. Three different classes of near-zero-parameter materials can be described as:

- ENZ (epsilon-near-zero) is the class of metamaterials whose relative permittivity is near zero.
- MNZ (mu-near-zero) is the class of metamaterials whose relative permeability is near zero.
- DNZ (Double-near-zero) is the type of metamaterials where both permittivity and permeability are near to zero.

ENZ mediais realized by electrically adding small metal particles in the dielectric material and DNZ mediums may be realized as tuned photonic crystal in order to obtained a Dirac-like cone dispersion at the τ-point in the photonic band structure [26] under some suitable conditions [27]. In order to realize (MNZ) medium with one component of permeability near to zero, the transmission-line metamaterials are used. The properties of an isotropic and inhomogeneous (MNZ) metamaterials are investigated in cylindrical and Cartesian coordinate system which show excellent potential results for transmission line in implementation of novel transmission optics devices [28]. The number of researchers have worked in near zero mediums such as ENZ slab and ENZ lens etc., to study the phase of fields in these mediums. The scattering widths of a circular cylinder coated with (ENZ) and (DNZ) mediums for normally incident plane wave studied for both TE and TM polarization, which shows TE polarization has steady phase as compared to TM polarization and found that the scattering widths were larger for dielectric-coated ENZ or DNZ cylinder and smaller for DNZ coated dielectric cylinder [29].

Here in this study, by using the SPM technique we will calculate scattered field by PEC slot embedded near zero index (NZI) metamaterials. A time dependency of $e^{-j\omega t}$ is assumed for the analysis.

INTERNATIONAL JOURNAL OF ADVANCED RESEARCH
International Peer-Reviewed Research Journal
ISSN (Online): 3106-7980 | ISSN (Print): 3106-7972
Volume 3 • Issue 2 • April 2026

Problem Formulation

The problem [1] is extended for the analysis of scattering width versus observation angle. The problem is formulated for the three different classes of near-zero-parameter materials (MNZ, ENZ, and DNZ). An electromagnetic plane wave with a unit amplitude, incident upon a PEC Slot of width 2d which is embedded in the near zero refractive index (NZI). The slot is formed by the two half-panes $y = 0, x > d$ and $y = 0, x < -d$. The edges of the slot are parallel to the z-axis of a cylindrical coordinate system (r, θ, z). The (r, θ) plane is the plane of incidence with the diffraction making an incident angle θ_0 with the positive x-axis. The time harmonic factor $\exp(-i\omega t)$ is assumed to be suppressed throughout the solution.

$$\Phi^0 = e^{jk(x\cos\theta_0 + y\sin\theta_0)}, (0 < \theta_0 < \pi) \quad (1)$$

Here $k = k_0(\varepsilon_r \mu_r)^{1/2}$ is wave number, where ε_r and μ_r are the relative permittivity and relative permeability of the near zero refractive index (NZI), k_0 is the wave number of free space.

An attempt has been made to evaluate the diffracted field in the half-space $y \geq 0$ as shown in fig.1. subject to the Fraunhofer condition $kr >> 1$ and $kr >> \rho^2$ where ρ is the characteristic parameter defined below.

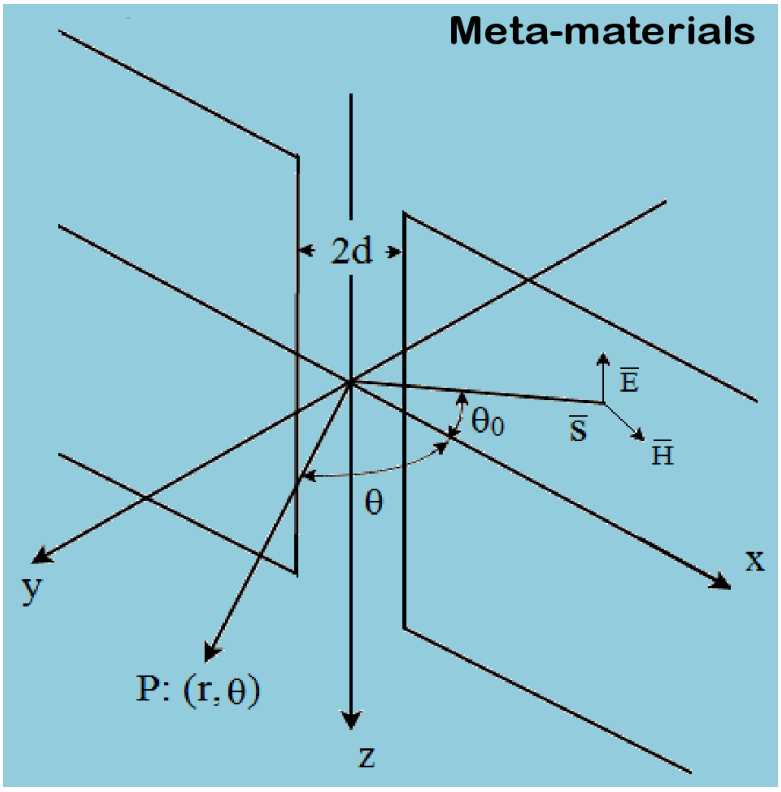


Figure 1: Diffraction of plane wave by the PEC Slot Embedded in NZI materials

$\rho = kd = 2\pi d/\lambda$
$d = width of the slot$
$r = the distance from the center$
$x = r\cos\theta$
$y = r\sin\theta$
$\alpha_0 = \cos\theta_0$
$\alpha = \cos\theta$

The diffracted field $\Phi = \Phi(x, y)$ is that solution of the wave equation

$$\frac{d^2\Phi}{dy^2} + \frac{d^2\Phi}{dx^2} + k^2\Phi = 0 \quad (2)$$

which satisfies the boundary condition $\Phi = 0$ for $y = 0, |x| > d$

and for the case $|x| < d)$ the following conditions of continuity must be satisfied,

$$\Phi(x,+0)=\Phi(x,-0),$$

$$\frac{\partial}{\partial y}\Phi(x,+0)=\frac{\partial}{\partial y}\Phi(x,-0)$$

Following Khaskind and Vainshteyn [3], diffracted field Φ is obtained as

$$\Phi=\Phi^0+\frac{1}{2\pi j}\int_{-\infty}^{\infty}\Psi(\alpha_0,\alpha)\frac{e^{jk\left[xa+|y|\sqrt{1-\alpha^2}\right]}}{\sqrt{1-\alpha^2}}d\alpha \quad (3)$$

where Ψ is given by,

$$\Psi(\alpha_0,\alpha)=\Psi(\alpha_0,\alpha)e^{-j\rho\alpha}+(-\alpha_0,-\alpha)e^{j\rho\alpha} \quad (4)$$

At a sufficiently great distance from the slot, the field decreases to a cylindrical wave in the upper half-space $y\geq 0$,

$$\Phi=\frac{\Psi(\alpha_0,\alpha)exp\left[j\left(kr-\frac{3\pi}{4}\right)\right]}{\sqrt{2\pi kr}} \quad (5)$$

The problem's solution [1] relies on two approximations: zero order and first order. Now if $\rho>>1$, the edge waves approach yields a zero-order solution, which is equivalent to the superposition of two waves coming from the half planes' edges. by applying the zero-order approximation in equation (5).

$$\Psi^0(\alpha_0,\alpha)=\Psi_0(\alpha_0,\alpha)e^{-j\rho\alpha}+\Psi_0(-\alpha_0,-\alpha)e^{j\rho\alpha} \quad (6)$$

the diffracted field takes the following simple form

$$\Phi=\frac{\sqrt{1+\alpha_0}\sqrt{1-\alpha}}{(\alpha-\alpha_0)\sqrt{2\pi kr}}\exp\left[j\left(\rho\alpha_0-\rho\alpha+kr-\frac{3\pi}{4}\right)\right]+\frac{\sqrt{1-\alpha_0}\sqrt{1+\alpha}}{(\alpha-\alpha_0)\sqrt{2\pi kr}}\exp\left[j\left(-\rho\alpha_0+\rho\alpha+kr-\frac{3\pi}{4}\right)\right] \quad (7)$$

Using the first order approximation in eq. (5)

$$\Psi^1(\alpha_0,\alpha)=\Psi_0(\alpha_0,\alpha)G(\rho,\alpha_0)G(\rho,-\alpha)e^{-j\rho\alpha}+\Psi_0(-\alpha_0,-\alpha)G(\rho,-\alpha_0)G(\rho,-\alpha)e^{j\rho\alpha} \quad (8)$$

the solution can be written as:

$$\Phi=\frac{\sqrt{1+\alpha_0}\sqrt{1-\alpha}}{(\alpha-\alpha_0)\sqrt{2\pi kr}}G(\rho,\alpha_0)G(\rho,-\alpha)\exp\left[j\left(\rho\alpha_0-\rho\alpha+kr-\frac{3\pi}{4}\right)\right]+\frac{\sqrt{1-\alpha_0}\sqrt{1+\alpha}}{(\alpha-\alpha_0)\sqrt{2\pi kr}}G(\rho,-\alpha_0)G(\rho,\alpha)\exp\left[j\left(-\rho\alpha_0+\rho\alpha+kr-\frac{3\pi}{4}\right)\right] \quad (9)$$

In this case, the cylindrical wave emitted by the edge $y=0,x=d$ is represented by the first term on the right side of the solution above and the second term represents the wave radiated by the edge $y=0,x=-d$. where G is the Sommerfeld Green's function and is given as follows,

$$G(\rho,\eta)=\sqrt{2}e^{-j\pi/4}\{C[2\sqrt{\pi\rho(1-\eta)}]+jS[2\sqrt{\pi\rho(1-\eta)}]\} \quad (10)$$

Here G and S are defined by the expressions

$$C(z)=\int_0^z\cos\frac{\pi}{2}t^2dt \quad (11)$$

And

$$S(z)=\int_0^z\sin\frac{\pi}{2}t^2dt \quad (12)$$

Above both integrals are the real and imaginary parts, respectively, of the complex Fresnel integral.

INTERNATIONAL JOURNAL OF ADVANCED RESEARCH
International Peer-Reviewed Research Journal
ISSN (Online): 3106-7980 | ISSN (Print): 3106-7972
Volume 3 • Issue 2 • April 2026

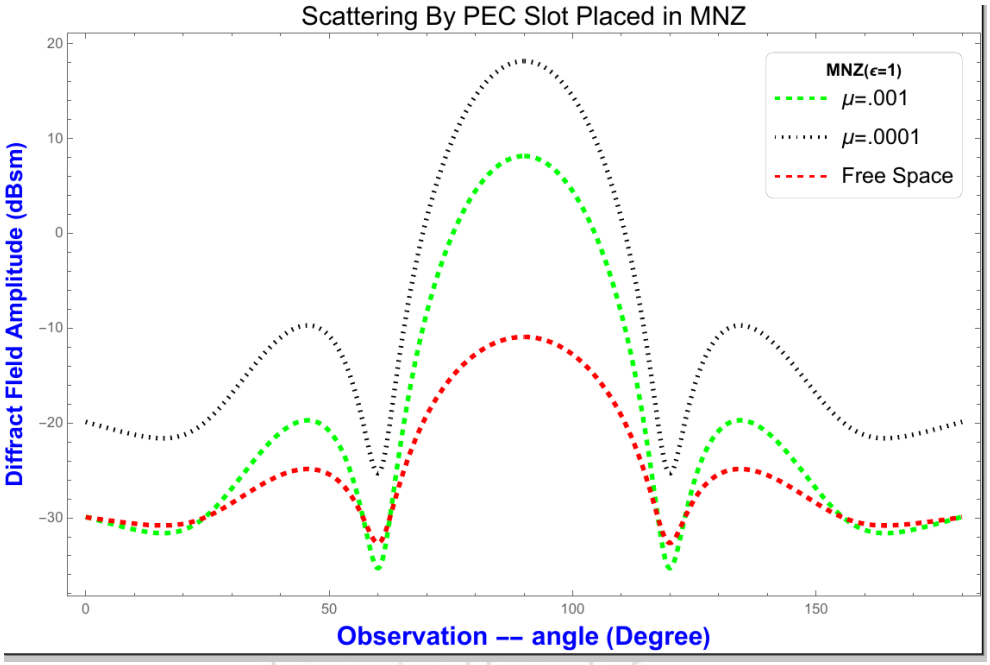


Figure 2: Diffracted Field by PEC Slot Embedded in MNZ Materials when $\boldsymbol{\varepsilon = 1}$ at incident angle $\boldsymbol{\phi = 90}$.

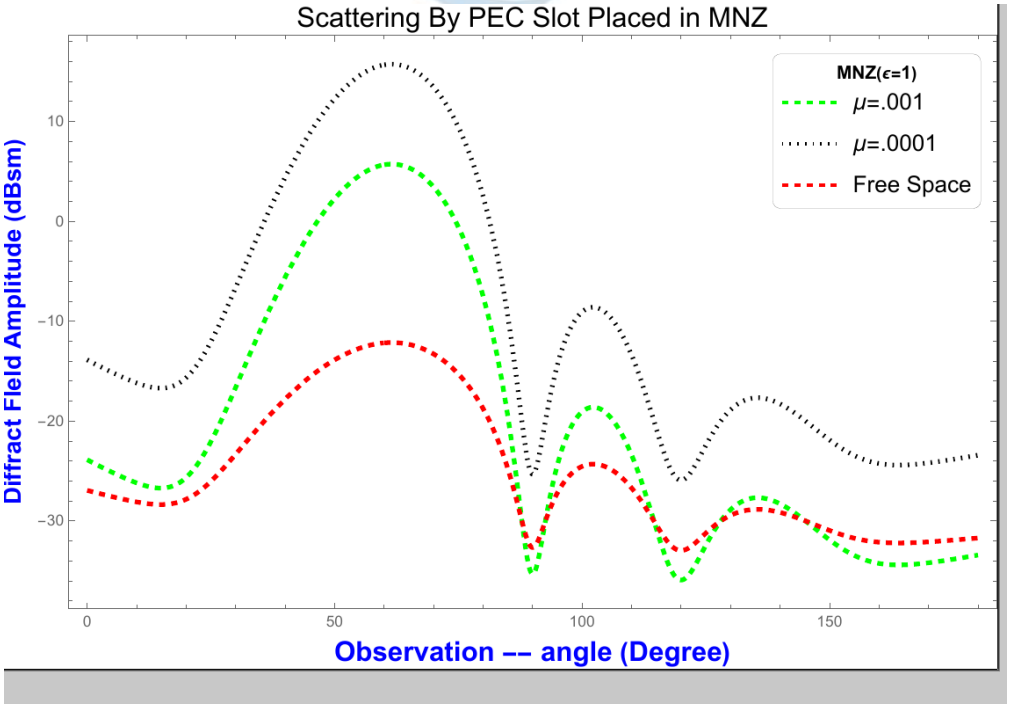


Figure 3: Diffracted Field by PEC Slot Embedded in MNZ Materials when $\boldsymbol{\varepsilon = 1}$ at incident angle $\boldsymbol{\phi = 60}$.

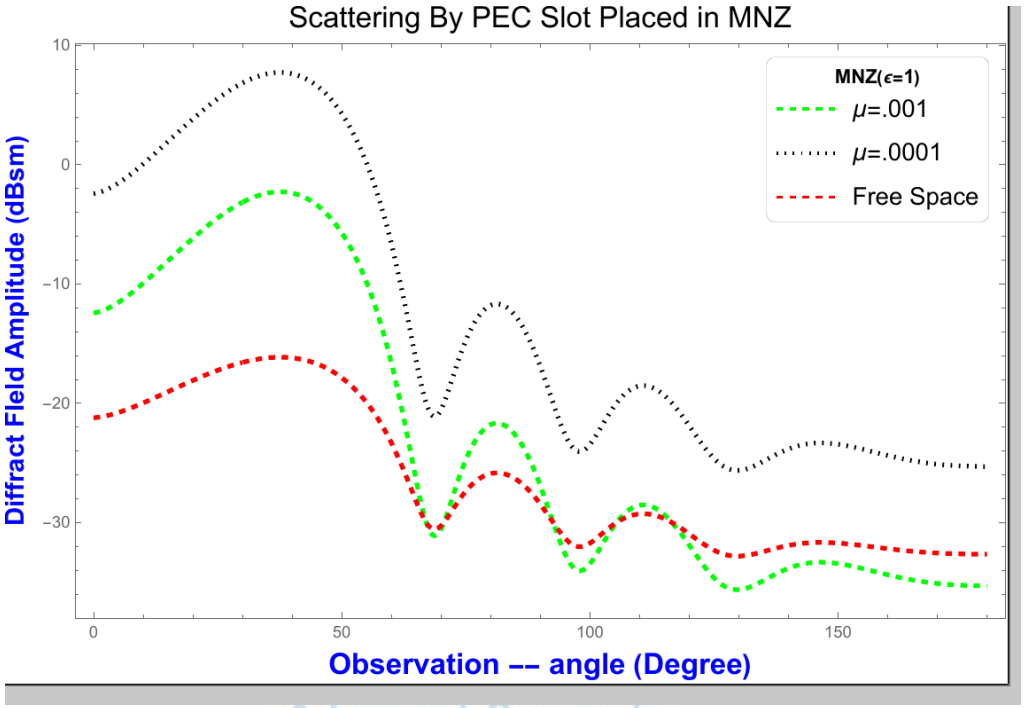


Figure 4: Diffracted Field by PEC Slot Embedded in MNZ Materials when $\varepsilon = 1$ at incident angle $\phi = 30$.

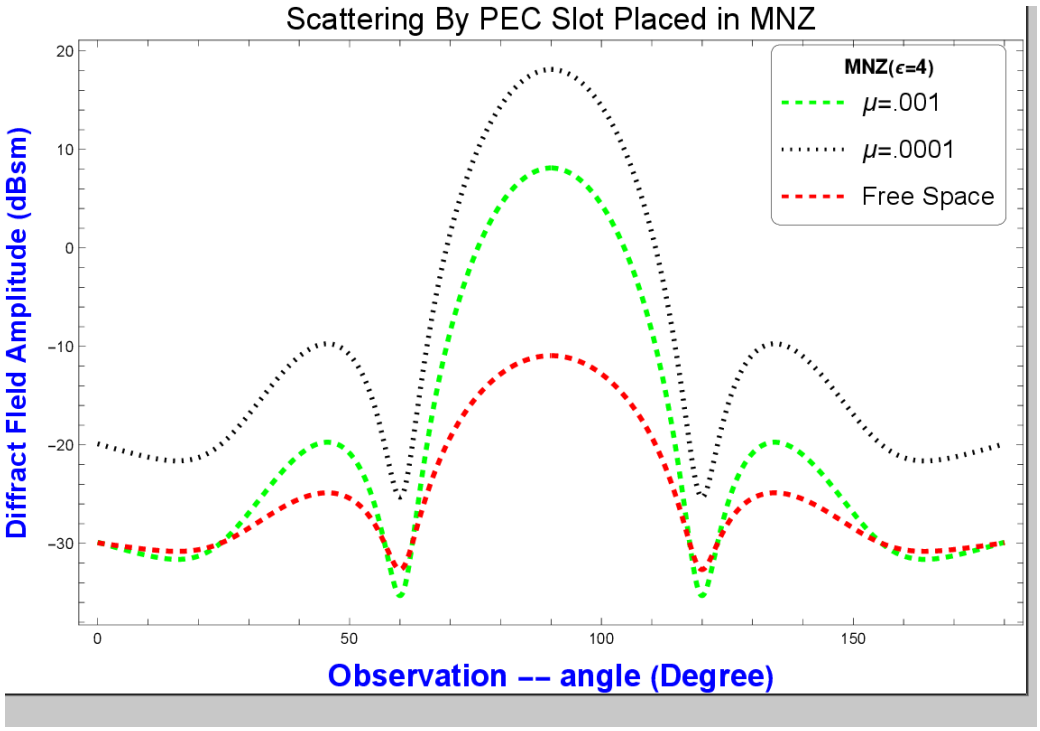


Figure 5: Diffracted Field by PEC Slot Embedded in MNZ Materials when $\varepsilon = 4$ at incident angle $\phi = 90$.

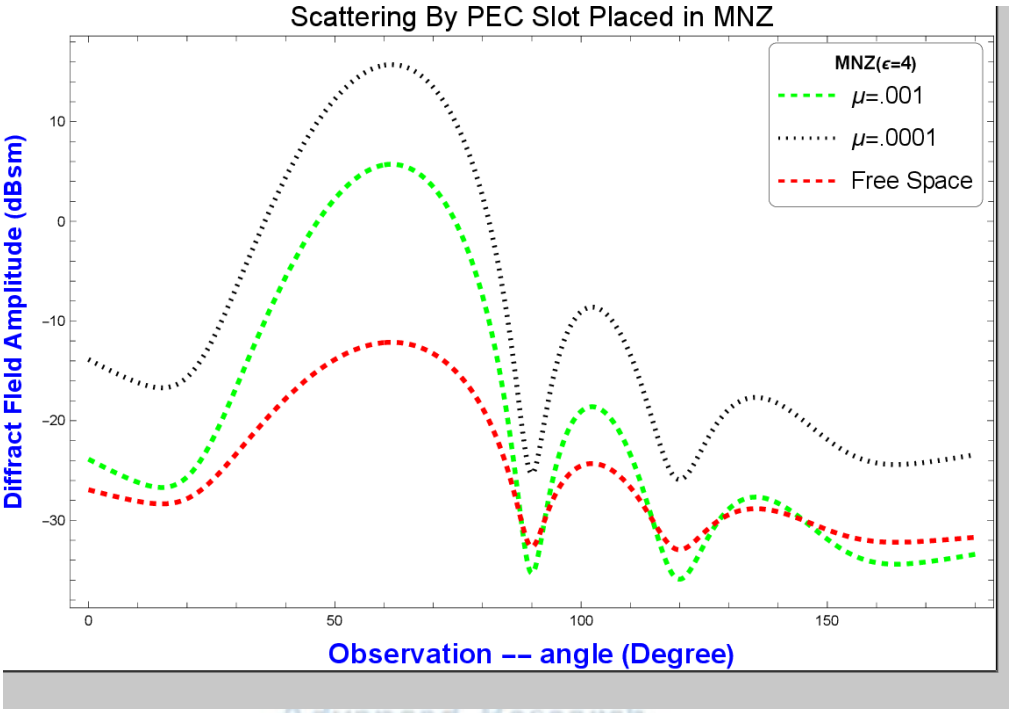


Figure 6: Diffracted Field by PEC Slot Embedded in MNZ Materials when $\boldsymbol{\varepsilon = 4}$ at incident angle $\boldsymbol{\phi =}$ **60.**

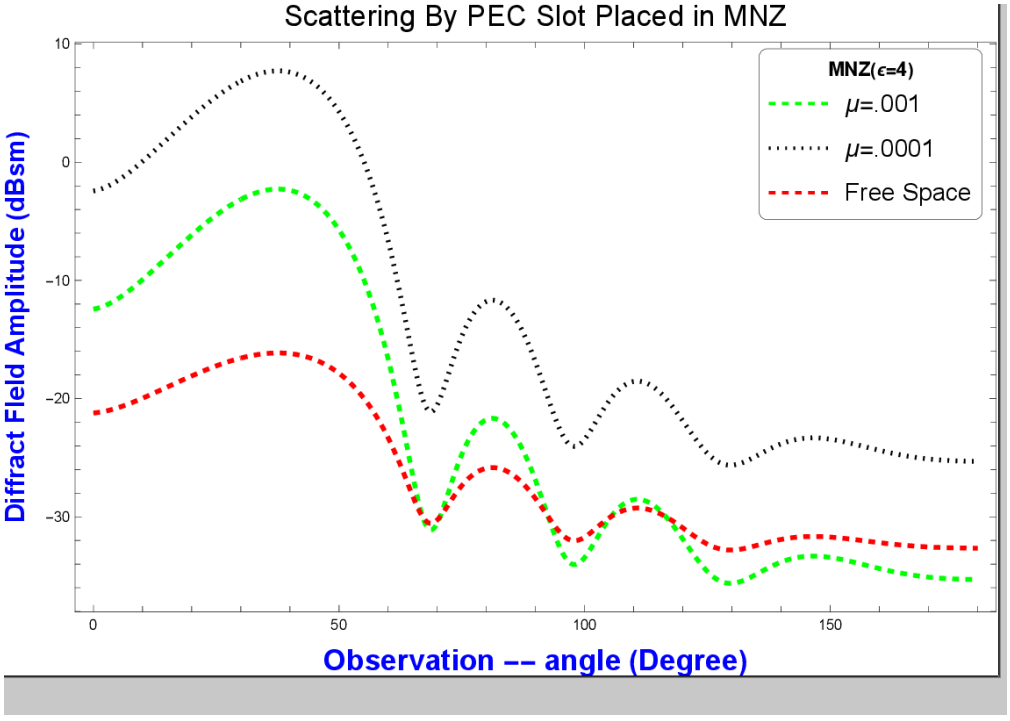


Figure 7: Diffracted Field by PEC Slot Embedded in MNZ Materials when $\boldsymbol{\varepsilon = 4}$ at incident angle $\boldsymbol{\phi =}$ **30.**

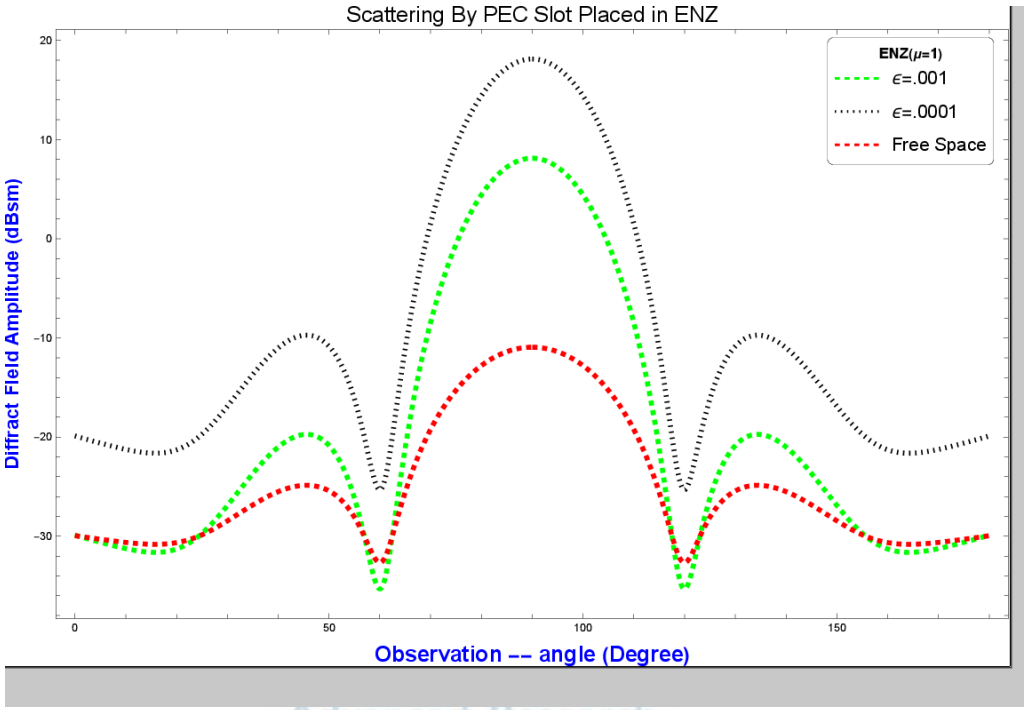


Figure 8: Diffracted Field by PEC Slot Embedded in ENZ Materials when $\mu = 1$ at incident angle $\phi = 90$.

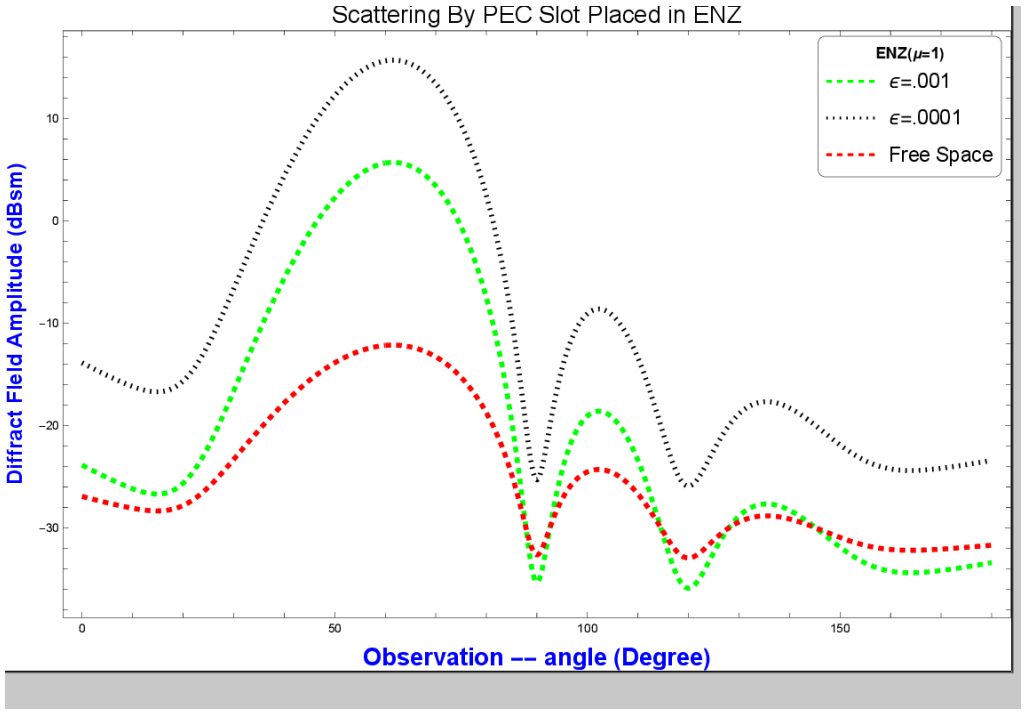


Figure 9: Diffracted Field by PEC Slot Embedded in ENZ Materials when $\mu = 1$ at incident angle $\phi = 60$.

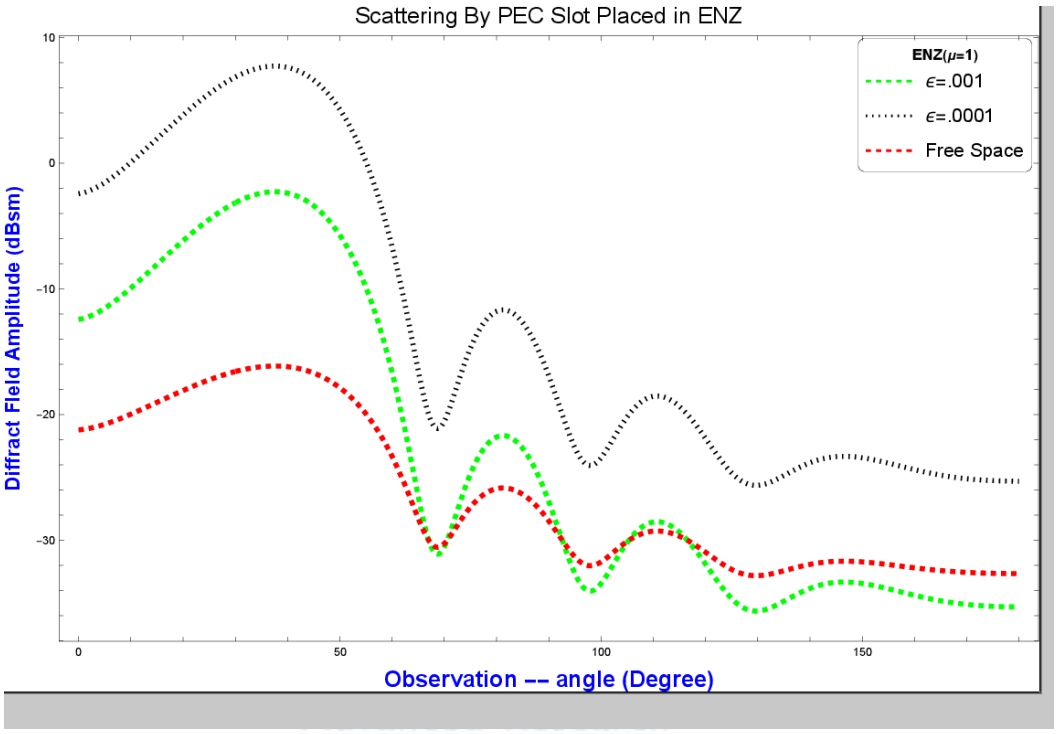


Figure 10: Diffracted Field by PEC Slot Embedded in ENZ Materials when $\mu = 1$ at incident angle $\phi = 30$.

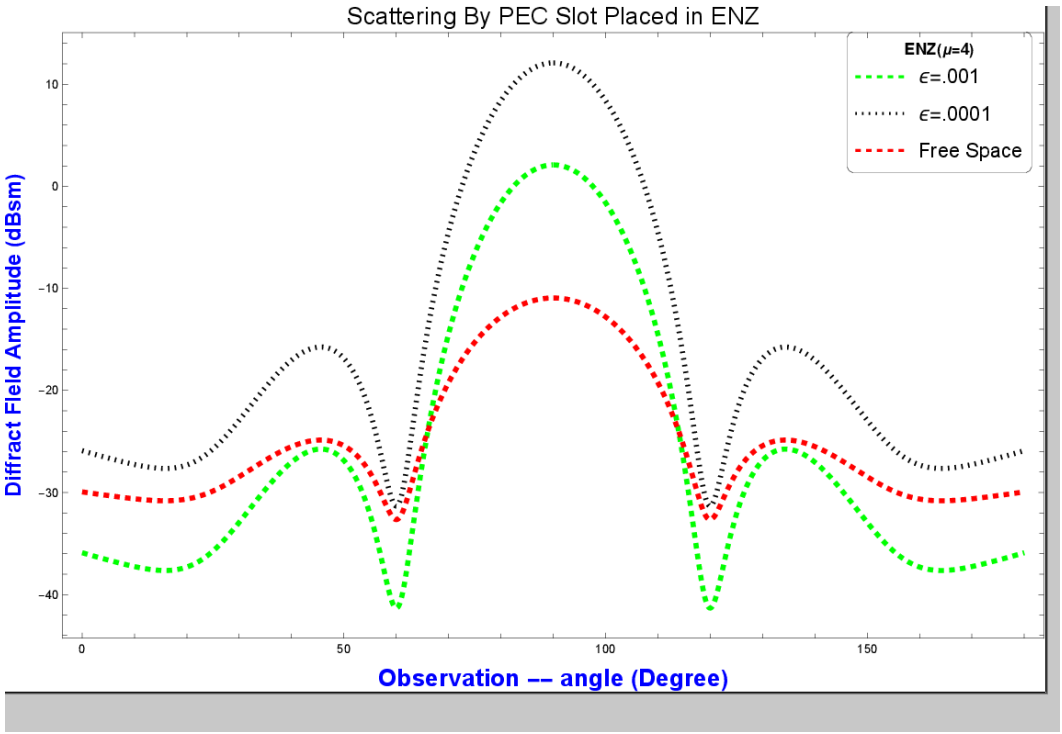


Figure 11: Diffracted Field by PEC Slot Embedded in ENZ Materials when $\mu = 4$ at incident angle $\phi = 90$.

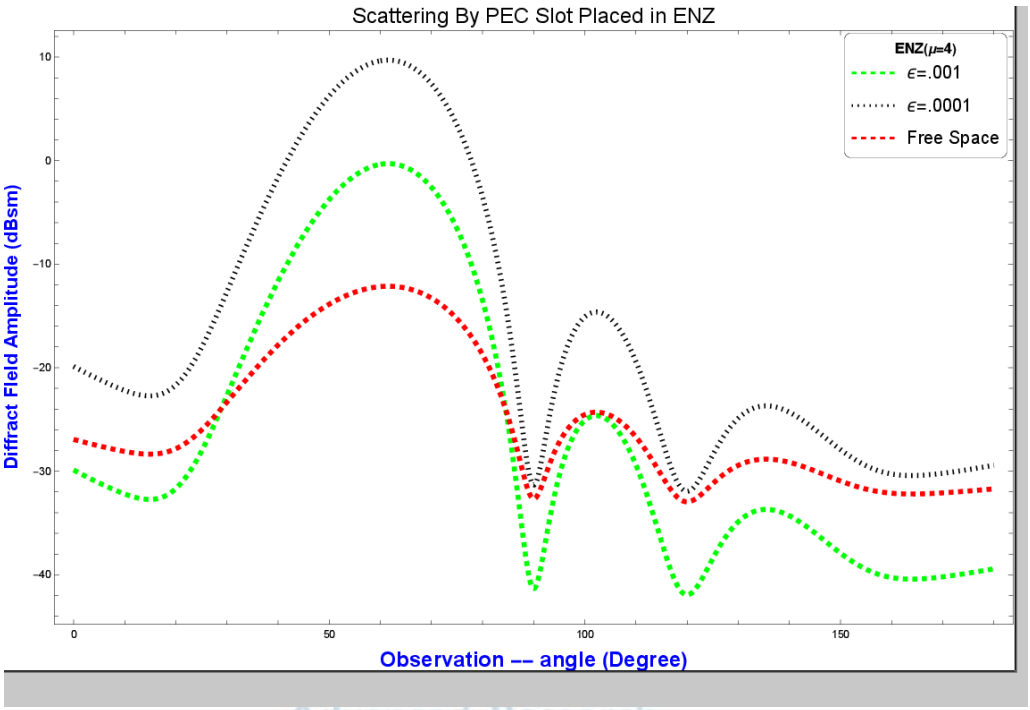


Figure 12: Diffracted Field by PEC Slot Embedded in ENZ Materials when $\mu = 4$ at incident angle $\phi = 60$.

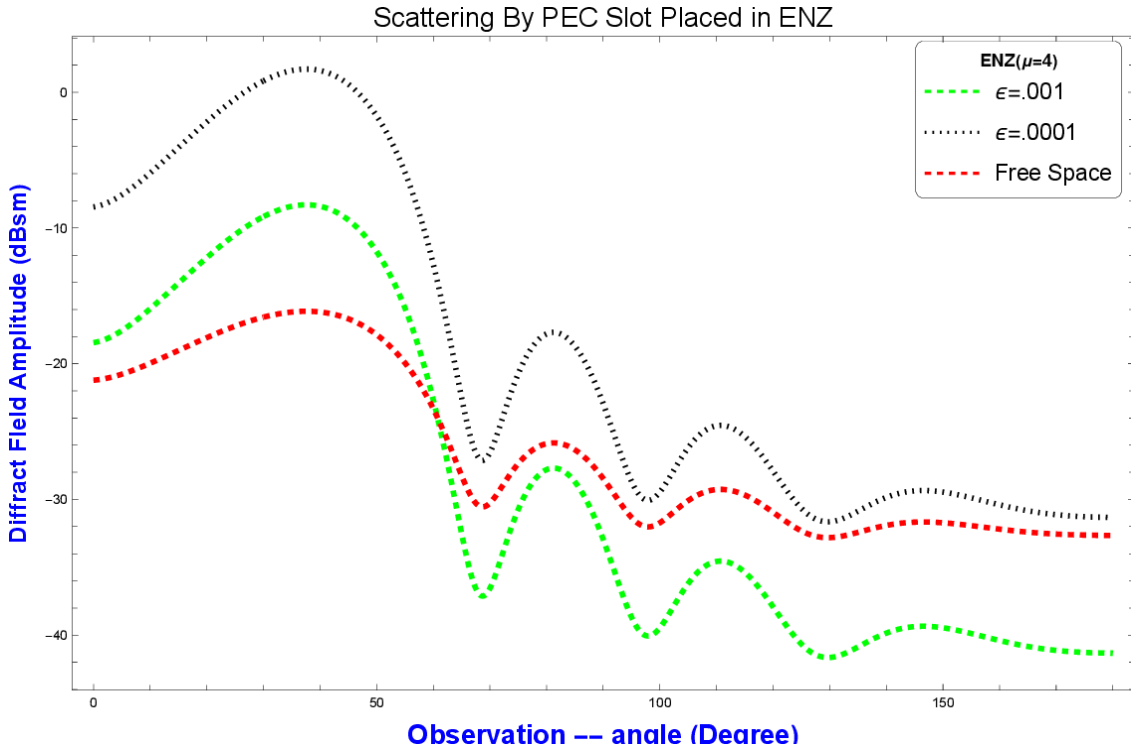


Figure 13: Diffracted Field by PEC Slot Embedded in ENZ Materials when $\mu = 4$ at incident angle $\phi = 30$.

INTERNATIONAL JOURNAL OF ADVANCED RESEARCH
International Peer-Reviewed Research Journal
ISSN (Online): 3106-7980 | ISSN (Print): 3106-7972
Volume 3 • Issue 2 • April 2026

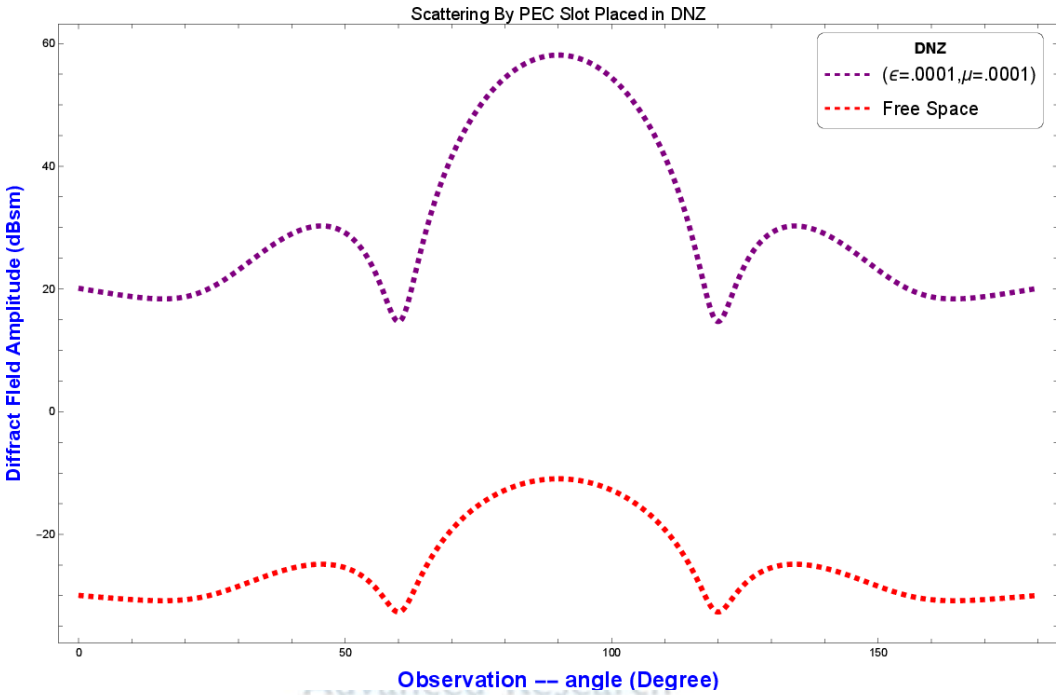


Figure 14: Diffracted Field by PEC Slot Embedded in DNZ Materials when $(\boldsymbol{\varepsilon} = .0001, \boldsymbol{\mu} = .0001)$ at incident angle $\boldsymbol{\phi} = 90$.

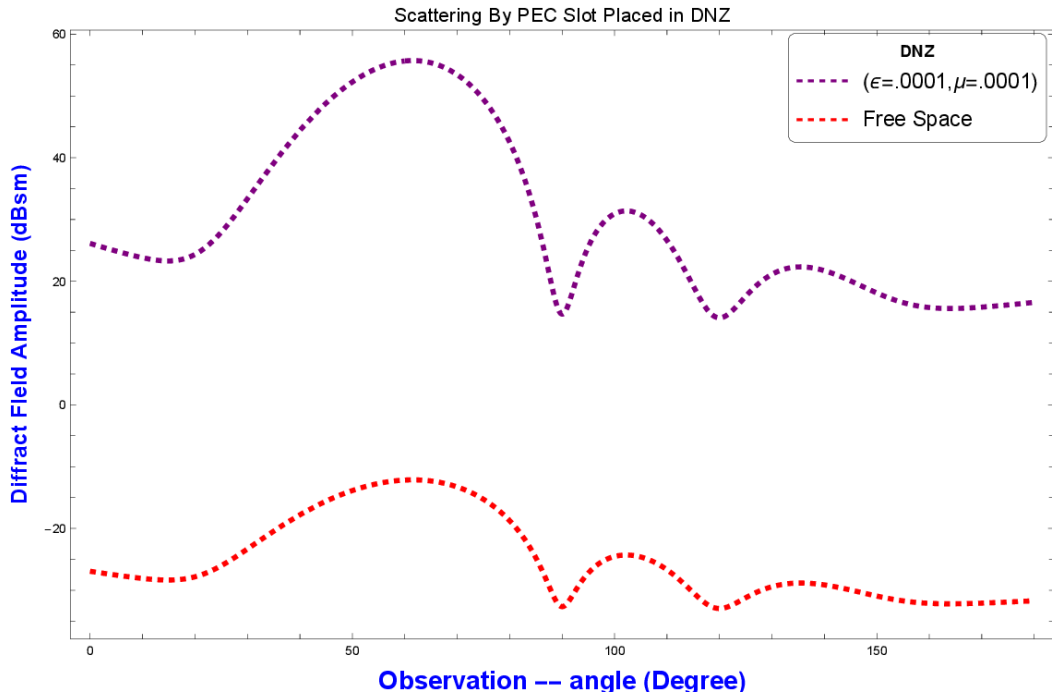


Figure 15: Diffracted Field by PEC Slot Embedded in DNZ Materials when $(\boldsymbol{\varepsilon} = .0001, \boldsymbol{\mu} = .0001)$ at incident angle $\boldsymbol{\phi} = 60$.

INTERNATIONAL JOURNAL OF ADVANCED RESEARCH
International Peer-Reviewed Research Journal
ISSN (Online): 3106-7980 | ISSN (Print): 3106-7972
Volume 3 • Issue 2 • April 2026

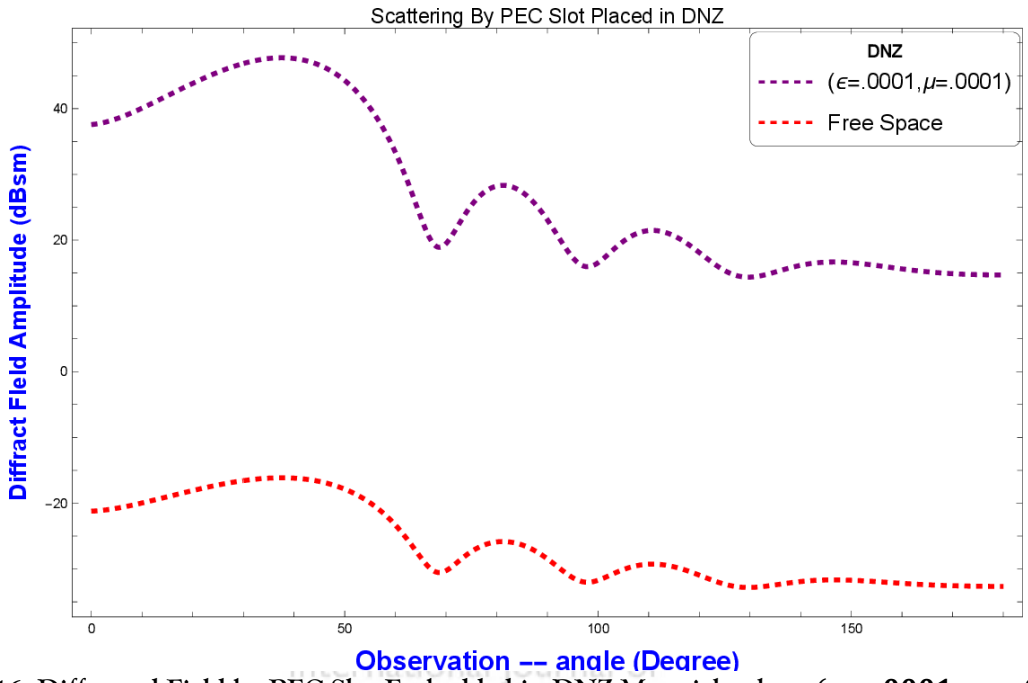


Figure 16: Diffracted Field by PEC Slot Embedded in DNZ Materials when $(\boldsymbol{\varepsilon} = .\mathbf{0001}, \boldsymbol{\mu} = .\mathbf{0001})$ at incident angle $\boldsymbol{\phi} = \mathbf{30}$.

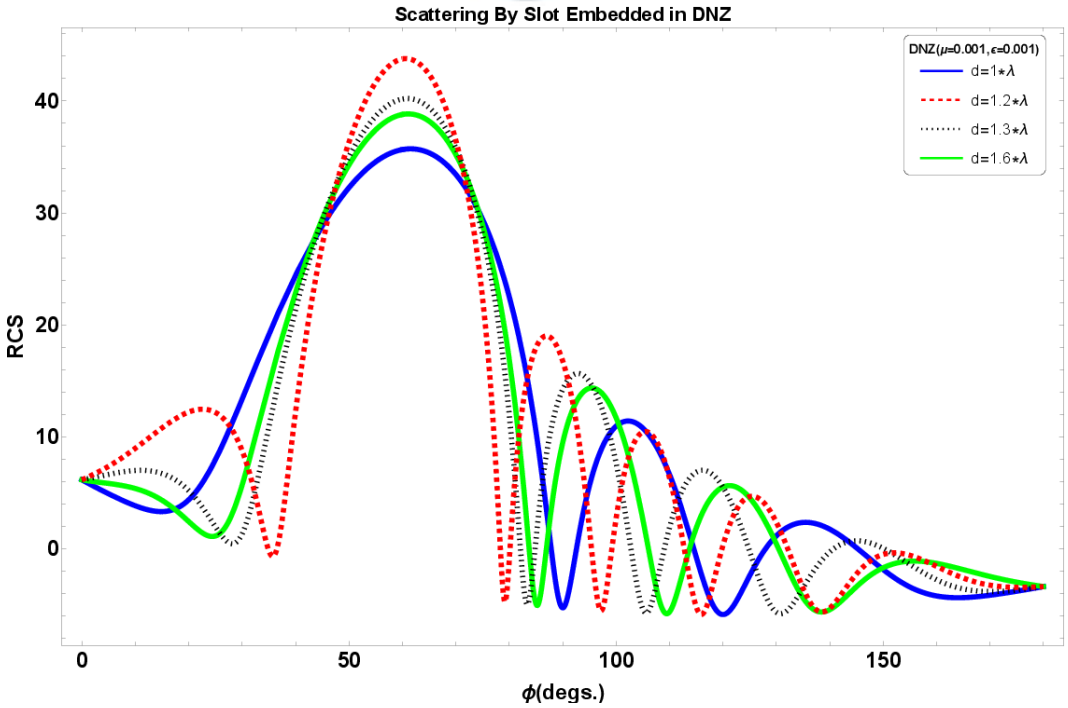


Figure 17: Diffracted Field by PEC Slot Embedded in DNZ Materials when $(\boldsymbol{\varepsilon} = .\mathbf{001}, \boldsymbol{\mu} = .\mathbf{001})$ for different widths of slot shown in the graph.

Numerical Results and Discussion

Using the theoretical results we have produced numerical results with self explainatory plots through Mathematica Software. We have compared the scattering field amplitude for MNZ, ENZ and DNZ near zero index metamaterials. We can see scattering field variation in the figure 2-16. As we increase near zero index using MNZ, ENZ and DNZ, the amplitude increases. Fig.1 shows the diffracted field by PEC Slot Embedded in MNZ Materials when $\varepsilon = 1$ at incident angle $\phi = 90$. Fig.2 shows the diffracted field by PEC Slot Embedded in MNZ Materials when $\varepsilon = 1$ at incident angle $\phi = 60$. Fig.3 shows the diffracted field by PEC Slot Embedded in MNZ Materials when $\varepsilon = 1$ at incident angle $\phi = 30$. Fig.4 shows the diffracted field by PEC Slot Embedded in MNZ Materials when $\varepsilon = 4$ at incident angle $\phi = 90$. Fig.5 shows the diffracted field by PEC Slot Embedded in MNZ Materials when $\varepsilon = 4$ at incident angle $\phi = 60$. Fig.6 shows the diffracted field by PEC Slot Embedded in MNZ Materials when $\varepsilon = 4$ at incident angle $\phi = 30$. Fig.7 shows the diffracted field by PEC Slot Embedded in ENZ Materials when $\mu = 1$ at incident angle $\phi = 90$. Fig.8 shows the diffracted field by PEC Slot Embedded in ENZ Materials when $\mu = 1$ at incident angle $\phi = 60$. Fig.9 shows the diffracted field by PEC Slot Embedded in ENZ Materials when $\mu = 1$ at incident angle $\phi = 30$. Fig.10 shows the diffracted field by PEC Slot Embedded in ENZ Materials when $\mu = 4$ at incident angle $\phi = 90$. Fig.11 shows the diffracted field by PEC Slot Embedded in ENZ Materials when $\mu = 4$ at incident angle $\phi = 60$. Fig.12 shows the diffracted field by PEC Slot Embedded in ENZ Materials when $\mu = 4$ at incident angle $\phi = 30$. Fig.13 shows the diffracted field by PEC Slot Embedded in DNZ Materials when $(\varepsilon = .0001, \mu = .0001)$ at incident angle $\phi = 90$. Fig.14 shows the diffracted field by PEC Slot Embedded in DNZ Materials when $(\varepsilon = .0001, \mu = .0001)$ at incident angle $\phi = 60$. Fig.15 shows the diffracted field by PEC Slot Embedded in DNZ Materials when $(\varepsilon = .0001, \mu = .0001)$ at incident angle $\phi = 30$.

Conclusion

It has been studied that the effects of MNZ, ENZ and DNZ materials on the diffracted field by PEC slot enhances the amplitude. Due to the DNZ medium clocking of the objects becomes visible . Counter measures of the stealth technology are attained, Radar can easily detect invisible objects by the signal enhancement. As the diffracted field is proportional to the size of the scatterers i.e. In the presence of DNZ background medium, the size of the slot becomes larger. This study can be helpful in detecting invisible cloaking. By enhancing the width of slot, angular width of the peak becomes narrow.

REFERENCES

[1] R. D. Jones, "diffraction of a planar electromagnetic Waves by a Slot", EMR/EMP Division 9353 (Technical Memorandum SLA-73-0657), Sandia Laboratories, Albuquerque, New Mexico 87115, 1973.

[2] S. N. Karp and A. Russek, J. Appl. Phys. 27, 886(1956).

[3] M. D. Khaskind and L. A. Vainshteyn, Rad. Eng. Electron, Phys. 9, 1492 (1964).

[4] J. B. Pendry, Negative refraction makes a perfect lens, *Physical review letters* 85 (18), 3966, 2000.

[5] A. AlÃ¹ and N. Engheta, Achieving transparency with plasmonic and metamaterial coatings, *Phys. Rev. E* 73, 019906, 2006.

[6] L. V. Alekseyev and E. Narimanov, Slow light and 3D imaging with non-magnetic negative index systems, *Optics Express* 14, 11184-11193, 2006

[7] H. K. Yuan, U. K. Chettiar, W. Cai, A. V. Kildishev, A. Boltasseva, V. P. Drachev, and V. M. Shalaev, A negative permeability material at red light, *Optics Express* 15 (3), 1076-1083, 2007

[8] V. G Veselago, Electrodynamics of substances with simultaneously negative values of ε and μ, *Soviet Physics Uspekhi.* 92, 517-526, 1964

[9] Sakoda, Kazuaki, Optical Properties of

Photonic Crystals, *Springer*, 258, 2004.

[10] S. A. Ramakrishna, Physics of negative refractive index materials, *Reports on Progress in Physics* 68(449), 2005.

[11] J. B. Pendry and D. R. Smith, The Quest for the Superlens, *Scientific American* 295, 60-67, 2006.

[12] J. Li, L. Zhou, C. T. Chan, and P. Sheng, Photonic Band Gap from a Stack of Positive and Negative Index Materials, *Phys. Rev. Lett.*. 90, 083901, 2003

[13] D. R. Smith, W. J. Padilla, D. C. Vier, S. C. N. Nasser and S. Schultz, Composite Medium with Simultaneously Negative Permeability and Permittivity, *Phys. Rev. Lett.*,84, 4184, 2000.

[14] X. Zhang and Y. Wu, Scheme for achieving coherent perfect absorption by anisotropic metamaterials, *Optics Express.* 25 (5), 4860-4874, 2017.

[15] W. Xu, L. Li, H. Y. Yao, T. Yeo and Q. Wu, Left-handed Material Effects on Waves Modes and Resonant Frequencies: Filled Waveguide Structures and Substrate-Loaded Patch Antennas, *Journal of Electromagnetic Waves and Applications.*, 2005.

[16] D. Schurig, J. J. Mock, B. J. Justice, S. A. Cummer, J. B. Pendry, A. F. Starr, D. R. Smith, Metamaterial Electromagnetic Cloak at Microwave Frequencies, *SCIENCE* 314, 977, 2006.

[17] R.W. Ziolkowski, Propagation in and scattering from a matched metamaterial having a zero index of refraction, *Phys. Rev. E.*, 70, 046608, 2004.

[18] A. Capretti, Y. Wang, N. Engheta, and L. D. Negro, Enhanced third-harmonic generation in Si-compatible epsilon-near-zero indium tin oxide nanolayers, *Optics Letters.* 40 (7), 1500-1503, 2015.

[19] J. Hao, W. Yan, and M. Qiua, Super-reflection and cloaking based on zero index metamaterial, *Appl. Phys. Lett* 96, 101109, 2010.

[20] E. Kallos, C. Argyros, Y. Hao, and A. AlÃ¹, Comparison of frequency responses of cloaking devices under nonmonochromatic illumination, *Phys. Rev. B.* 84, 045102, 2011.

[21] P. Y. Chen, C. Argyropoulos, and A. AlÃ¹, Broadening the Cloaking Bandwidth with Non-Foster Metasurfaces, *Phys. Rev. Lett..* 111, 233001, 2013.

[22] K. Konstantinidis1 and A. P. Feresidis, Broadband near-zero index metamaterials, *J. Opt.* 17, 105104, 2015.

[23] H. F. Ma, J. H. Shi, B. G. Cai and T. J. Cui, Total transmission and super reflection realized by anisotropic zero-index materials, *New J. Phys.* 14 123010, 2012.

[24] B. Edwards, A. AlÃ¹, M. E. Young, M. Silveirinha, and N. Engheta, Experimental Verification of Epsilon-Near-Zero Metamaterial Coupling and Energy Squeezing Using a Microwave Waveguide, *Phys. Rev. Lett.* 100, 033903, 2008.

[25] Y. Yuan, N. Wang and J. H. Lim, On the omnidirectional radiation via radially anisotropic zero-index metamaterials, *EPL* 100, 34005, 2012.

[26] A. M. Mahmoud, N. Engheta, Wave-matter interactions in epsilon-and-mu-near-zero structures, *Nat Commun*, 25476550, 2014.

[31] F. Tehreem, M. A. Fiaz, M. Faryad, On the planewave scattering from a circular cylinder with core or coating made of ENZ and DNZ mediums, *Journal of Physics Communications* 2(11), 115025, 2018.

[27] M. W. Ashraf and M. Faryad, On the mapping of Dirac-like cone dispersion in dielectric photonic crystals to an effective zero-index medium, *Journal of the Optical Society of America B* 33(6), 1008-1013, 2016.

[28] A. H. Huang, Q. Cheng, Realization of Mu-Near-Zero medium by transmission-line metamaterials, *IEEE.*, 16124963, 2016.

[29] S. O. Rice, Reflection of electromagnetic waves from slightly rough surfaces, *Communications on pure and applied mathematics.* 4, 351-378, 1951.